

Flight performance modeling to optimize trajectories

J. Rosenow and H. Fricke, Technische Universität Dresden, Institut für Luftfahrt und Logistik, 01062 Dresden, Germany
{Judith.Rosenow,Hartmut.Fricke}@tu-dresden.de

Abstract

Along the ambitious SESAR objectives, new aircraft performance models are necessary to calculate and optimize free route aircraft specific trajectories considering real weather conditions. Here, an aircraft performance model is presented, which meets these requirements. To consider constant changes in speed and acceleration, the dynamic equation of this unsteady system is solved analytically. Free variables are controlled by an aircraft specific proportional plus integral plus derivative controller. Therewith, the model is based solely on physical functions (except for the drag polar, which is approximated by BADA) and calculates only physically possible trajectories. Several aircraft and engine types are included, the aircraft specific behavior can be modeled in detail and emissions can be quantified. Trajectory optimization is demonstrated by a variation of the cruising altitude and the target speed. Both are effective variables. We found, that the developed optimization target function cannot be generalized for all aircraft types, especially not under real weather conditions. Individual aircraft specific target functions mainly depend on the drag polar, the maximum Mach number and the operating empty weight.

1. INTRODUCTION

1.1. Motivation

The growing public awareness of the aviation impact on climate change forces aviation stakeholders more and more to search for climate friendly solutions. Optimization potential has been found on several air traffic planning levels ranging from network design to fleet assignment and trajectory optimization [1]. Regardless of the planning level, flight performance modeling is necessary for a reliable optimization of the air traffic system, because it is the smallest unit, on which each air traffic optimization should be based.

Since the foundation of the Single European Sky (SES) and the corresponding research program Single European Sky ATM Research (SESAR) in 1999, the reduction of the air traffic environmental impact is regulated by law [2]. In the SES Basic Regulation No 549/2014 [2] the objectives of SESAR are published aiming a warranty of a sustainable development of the European air traffic sector. Beside the triplication of capacity, the increase of safety by a factor of 10 and the decrease of air traffic management costs by 50 %, the environmental compatibility of each flight should be reduced by 10 %.

With the SESAR Masterplan the basic concept for the design of the future air traffic management (ATM) had been established by EUROCONTROL in 2012 to meet the SESAR targets by the introduction of an optimized flight trajectory [3]. Therein, the SESAR targets shall be carried out by "Moving from Airspace to 4D Trajectory Management". The first step towards this action is called the "Time-based operations" and focusses on the deployment of airborne trajectories [3], which considers all constraints inflicted by the highly complex and dynamic environmental conditions [4]. Free routing is also targeted

in this step, to enable optimized trajectories [3]. Free routes are freely planed routes between a defined entry point and a defined exit point constraint by published or unpublished waypoints [3]. These waypoints should originate from a multiobjective trajectory optimization considering the aircraft flight performance, its emissions and external influences like weather conditions. Hence, a target function for each objective is necessary. For this purpose, the Compromised Aircraft performance model with Limited Accuracy (COALA) has been developed, which derives the target figure (i.e. the true airspeed v_{TAS}) from target functions and controls the v_{TAS} with a proportional–integral–derivative controller. The 4D trajectory is achieved by the integration of the dynamic equation.

COALA has been developed in the framework of the research project MEFUL, where an optimum between the reduction of the aviation environmental impact and the costs is estimated on different planning levels, ranging from the individual trajectory up to the network structure [1]. This optimization is realized by a simulation environment called TOolchain for Multicriteria Aircraft Trajectory Optimization (TOMATO) [5], which evaluates the simulated air traffic system by using several sub models (COALA amongst others) and varies their input parameters until an optimum is reached.

1.2. State of the art

Flight performance can be modeled with different granularity depending on the intended use. For the sake of precise flight performance modelling, preferably for lots of aircraft types, plenty of sensitive parameters regarding aircraft specific aerodynamical parameters and the boundary conditions given by real atmospherical parameters have to be considered. In an ISA standard atmosphere, performance models are available for airlines, e.g. the commercial flight planning tool Lido/Flight 4D by Lufthansa Systems [6], with unknown precision and no

availability for universities. Furthermore, the Base of Aircraft Data (BADA) by the European Organization for the Safety of Air Navigation (EUROCONTROL) [7] [8] provides specific aircraft performance parameters and allows a performance modelling for a wide range of aircraft types. Some missing dependencies as compressibility effects in the calculation of the drag coefficient had been considered by Kaiser [9] resulting in a more precise modeling of the aircraft performance, the Enhanced Jet Performance Model (EJPM). This model had been used and applied for several problems, for example for estimations of the energy share of kinetic and potential energy during continuous descent operations [10], for considerations of flight profiles without contrail formation [11], for the influence of aircraft performance properties on the contrail life cycle [12], for automated trajectories [10] [13] and for synchronization of automated arrivals [14]. The target functions for optimization and some of the aerodynamic equations of the EJPM are used in COALA. Soler et al. [15] modeled the flight performance with a 3-degree-of-freedom dynamic model depending on v_{TAS} , heading and flightpath angle in an ISA atmosphere, but with two dimensional wind information from a national weather service. They only allowed flight levels during cruise, with a separation of 1000 feet. Hence, an optimum cannot be detected. However, all these applications use a single target function (e.g. minimum fuel flow or minimum time) for the optimization, which seems insufficient with the conflictive SESAR targets in mind. Furthermore, these models depend on defined waypoints, which must be flown with a most efficient performance. Still, the difficulty is to define the optimized waypoints.

Multi-criteria optimization of trajectories in a horizontal plane has been done by Sridhar et al. [16] under real weather conditions with a detailed horizontal flight performance modeling as a two point boundary value problem. Patrón et al. [17] and Murieta Mendoza [18] used multi-level optimizations in 3-D grid models. Anyhow, the flight performance is only approximated by a Performance database, where fuel burn and the distance traveled is calculated depending on Mach number (or Indicated Air Speed (IAS)), gross weight, temperature deviation of the ISA standard atmosphere and altitude. This approach only considers the reduction of fuel consumption or time of flight. Both Ringerz [19] and Howe-Veenstra [20] developed smooth optimized trajectories following constant IAS or constant Mach number and a constant altitude at cruise with a single, but variable target function considering a temperature deviation of the ISA standard atmosphere. Hargraves [21], Bittner [22] and Göttlicher [23] optimized trajectories as an optimal control problem, which is able to consider conflictive target functions and real weather conditions. The discrete input parameters are approximated by analytically solvable functions. From this follows, that only a restricted number of parameters can be considered and sometimes the errors done by the approximation seem too high. Furthermore, the flight performance is modeled in a very simple way.

The research project REACT4C of the German national aeronautics and space research center (DLR) published interesting findings regarding ecological trajectory optimization [24], [25], [26] and [27]. However, all these approaches can not be generalised due to the major impact of the assumed atmospheric conditions.

2. FLIGHT PERFORMANCE METHODOLOGY

2.1. Principle model function

With the 4D flight performance model COALA, we combined the impact of aircraft specific aerodynamics and the important influence of three dimensional weather information both affecting an optimized trajectory in the actual operational flight. COALA considers plenty of sensitive parameters. On the one hand, the flight performance is described by v_{TAS} , thrust, fuel flow, forces of acceleration, time of flight, and emission quantities. On the other hand, aircraft type specific aerodynamical parameters like wing area S , maximum Mach number MMO , number of engines, aircraft weights and the drag polar depending on flap handle position and Mach number are considered.

For the multicriterial optimization COALA uses target functions for v_{TAS} and flight path angle γ , which are continuously calculated for each time step and used as controlled variable and are controlled by using an aircraft specific proportional plus integral plus derivative controller (PID controller), with the lift coefficient as regulating variable. Aerodynamic and flight performance specific limits are considered all the time. Under real weather conditions the aircraft performance modeling turns into an unsteady system, because speed and acceleration are subject to constant changes, which are not negligible. Therewith, forces of acceleration have to be considered and minimized all the time.

According to [28] the dynamic equations in the horizontal plane (1) and in the vertical plane (2) are

$$F_T \cos \gamma - F_A \sin \gamma - F_W \cos \gamma = m \cdot a_x \quad (1)$$

$$F_A \cos \gamma + F_T \sin \gamma - F_G - F_W \sin \gamma = m \cdot a_y \quad (2)$$

where F_T denotes thrust [N], F_A lift [N], F_W drag, F_G the aircraft weight [N], m the aircraft mass [kg] and a_x , a_y the acceleration [m/s²] in the horizontal and vertical plane, respectively. γ represents the flight path angle [rad] and is defined as [28]

$$\gamma = \arctan\left(\frac{F_T}{F_A} - \frac{c_w}{c_A}\right). \quad (3)$$

In Equation (3), c_w and c_A denote the drag coefficient [a.u.] and lift coefficient [a.u.], describing F_A and F_W in the following way [28]:

$$F_A = \frac{\rho}{2} v_{TAS}^2 S c_A \quad (4)$$

$$F_W = \frac{\rho}{2} v_{TAS}^2 S c_w. \quad (5)$$

The lift coefficient c_A is used as regulative variable in the PID controller and the drag coefficient c_w is calculated as function of Mach number, flap position and lift coefficient according to BADA. In general, the BADA revision 4.1 [7] is used, unless the aircraft is not included. Otherwise, the BADA model 3.6 [8] is used. The accelerations a_x and a_y are integrated for the estimation of the ground speed and

ground distance. A time resolution of $dt = 1$ s turned out to be sufficient. True airspeed and air distance are calculated by considering wind direction and wind speed.

2.2. Input parameters

The weather data with variable spatial resolution are taken from grib2 (GRIdded Binary) data, provided by the National Weather Service NOAA [29]. Weather data between the given weather data points are achieved by linear interpolation. The following weather data are used: Temperature T [K], air density ρ [kg/m³], pressure p [Pa], wind speed for Eastward u and Northward v directions and relative humidity rH [a.u.]. Alternatively, COALA can deal with one dimensional weather information in form of a standard atmosphere.

In case of three dimensional weather information, COALA needs the lateral flightpath, given in geographical coordinates (longitude and latitude) at an adequate number of sampling points. Between these supporting points, the flightpath is calculated by linear interpolation. Hence, spiraling is not included yet. In case of one dimensional weather information, the distance between start and destination is sufficient.

COALA considers plenty of aircraft specific data, some of which are taken from other models. Beside the aircraft type the take-off weight [kg], as sum of operating empty weight OEW [kg], payload [kg] and fuel mass [kg], the maximum Mach number MMO , the wing area, the service ceiling as maximum cruise altitude, are considered. Additionally, some engine specific information are required to calculate the emissions with the highest possible accuracy according to [30], [31] and [32]. Therefore, the engine pressure ratio, the bypass ratio and the reference emission quantities for carbon monoxides, unburned hydrocarbons, nitric oxides, and soot number depending on a thrust setting specific fuel flow are taken from the ICAO Aircraft Engine Emissions Databank provided by EASA [33].

2.3. Take-off

For take-off, the lift coefficient c_A depending on flap position and angle of attack α is linearly approximated. Furthermore, cross wind is neglected. The take-off thrust is achieved by a linear interpolation between maximum climb thrust MCL , if the aircraft weight corresponds with OEW and maximum take-off thrust MTO

$$MTO = 1.3 \cdot MCL \quad (6)$$

if the maximum take-off weight $MTOW$ is reached. MCL is calculated with BADA [7] [8]. The coefficient of rolling resistance is set to $\mu_r = 0.03$, which corresponds to tires of large trucks on asphalt [34]. The rotation speed v_r is defined where lift F_A exceeds weight F_G by 30 %, assuming a lift coefficient $c_A(\alpha = 10^\circ)$.

2.4. Climb

Climb is operated as continuous climb operation without any steps [35]. Climb is divided into two phases as stated in [1]. First, a climb with maximum angle of climb γ is used below 10000 ft altitude. The aspired true air speed v_{TAS} is

calculated by a extremum determination of Equation (1) and (2) in form

$$F_T = \frac{\rho}{2} v_{TAS}^2 \cdot S \cdot c_W + m \cdot g \cdot \sin \gamma + m \cdot a \quad (7)$$

where a is the acceleration projected on the flight path. The drag coefficient c_W is estimated according to BADA [7] [8] and the lift coefficient is used as regulative variable in the PID controller to achieve the aspired v_{TAS} . This first climb phase aims in a geometrically steepest climb [36] to reach the safety altitude (10000 ft) without investing in kinetic energy. Between three and five minutes after start, thrust is linearly reduced to MCL , which is used vor the remaining climb phase.

Above 10000 ft a new target function for v_{TAS} is used, where the climb rate w

$$w = \sin \gamma \cdot v_{TAS} \quad (8)$$

is maximized in Equation (7). Therewith, the maximum gain in altitude per time unit is utilized [36]. The cost index CI of this steep climb flight converges to $CI = 0$, the aircraft invests the maximum amount of the energy in potential energy, because flying at cruising altitude is more fuel efficient.

To achieve climb gradients different from the steepest possible ones, the target value of v_{TAS} can be increased resulting in a shallower climb angle, because more energy is converted into kinetic energy. This speed adjustment is realized by a variable factor α . Therewith, trajectories with shorter time of flight, but increased fuel flow (i.e. $CI > 0$) can be generated.

2.5. Cruise

In COALA, cruise begins, when the aspired cruising pressure altitude p_{cruise} or geometrical altitude h_{cruise} is reached. Even during cruise, especially under real weather conditions, the aircraft performance model COALA describes an unsteady system, because speed and acceleration are still constantly changing. Hence, Equation (7) has to be solved for every time step. During cruise, again v_{TAS} is controlled with a PID controller. The target value of v_{TAS} is gained from a target function, which is the maximum of the specific range R_{spec} [9] calculated with Equation (7)

$$R_{spec} = \frac{v_{TAS}}{m_f} \quad (9)$$

With this method, a maximum gain in $v_{TAS,R_{spec}}$ per unit rate of fuel flow m_f [kg/s] is achieved. The required thrust F_T is estimated from Equation (7), for the target v_{TAS} assuming a stationary equilibrium (i.e. $F_A = F_G$). F_T will be increased, if the target pressure altitude can not be reached. In case of BADA 3.6 [8], maximum cruise thrust is $MCRZ = 0.95 \cdot MCL$, in BADA 4.1 [7], $MCRZ$ is equal to MCL . The target function results in a fuel minimized trajectory. As described for the climb phase, the target v_{TAS} can be increased by a constant factor α , resulting in a trajectory with $CI > 0$. The consequences of this speed adjustment will be discussed later.

In case of a standard atmosphere, the optimum pressure altitude p_{R_spec} can be calculated by replacing atmospheric parameters in Equation (7) (and functional relationships therein) by functions describing the standard atmosphere. Under real weather conditions, p_{R_spec} differs for every time step dt , due to the interpolation between the grid points with grib2 weather data. Hence, the flight would not be feasible. Considering real weather, a pressure altitude is expected as input parameter.

2.6. Descent

Descent is executed as continuous descent operation [37] down to the final approach fix in 10000 ft altitude. Approach, flare and landing are not implemented yet, because these phases do not pose a potential for optimization, due to strict safety regulations.

The top of descent (TOD) is already iteratively calculated during cruise, considering the actual aircraft weight and v_{TAS} and the corresponding rate of descent. As soon as the aircraft reaches the aspired distance or geographical coordinate, the descent flight will be initiated.

During descent, the engines operate in idle mode with $F_T = 0$ N and fuel flow is taken from BADA [7] [8]. The target value for v_{TAS} is continuously derived from an extremum determination of the lift to drag ratio E

$$E = \frac{F_A}{F_W}. \quad (9)$$

Again, v_{TAS} is controlled by a PID controller and regulated with the lift coefficient c_A . The resulting angle of descent is calculated following Equation (3) and the descent rate w is estimated with the use of Equation (8) (climb rate w).

2.7. Output parameters

COALA calculates the trajectory with fixed time steps and generates all relevant information for each time step. The 4D trajectory is generated for both the aerodynamic and the Earth-fixed coordinate system. Engine specific data as fuel flow and the engine emissions of carbon dioxide CO_2 , water vapor H_2O , nitric oxides NO_x , soot, sulfur oxides SO_2 , sulfuric acid H_2SO_4 , carbon monoxides CO and unburned hydrocarbons HC are calculated. The products of complete combustion CO_2 , H_2O , SO_2 and H_2SO_4 are estimated proportional to the fuel flow according to Lee et al. [30]. The products of incomplete combustion NO_x , CO and HC are calculated by using the state of the art Boeing-2 Fuel Flow method as described by Schäfer [32]. For the quantification of the soot emissions, an engine model providing the required combustor inlet temperature T_3 and pressure p_3 is used, as published by Kugele et al. [31].

3. RESULTS

To show the characteristics and prospects of COALA, a given lateral flight path from Frankfurt (EDDF) to Dubai (OMDB) with weather data from 2016, February, 2nd, 12 a.m. is used for two different air freighter, Boeing B777F and McDonnell Douglas MD-11F. Table 1 shows the most relevant characteristics of both aircrafts. For the B777F,

BADA 4.1 [7] data and for the MD-11F, BADA 3.6 [8] data is used.

Table 1: Characteristics of the modeled aircrafts. Data are taken from [8] and [7]. The following abbreviations are used: operating empty weight (OEW), maximum take-off weight (MTOW), Maximum range, fully loaded (R_{max}), maximum operating Mach number (MMO).

	B777F	MD-11F
OEW	145150 kg	112748 kg
MTOW	347452 kg	273300 kg
R_{max}	9.070 km	12.633 km
Engines	2 x GE-90 110B1L	3 x CF680C2D1F
Thrust	985200 N	809880 N
MMO	0.87	0.87
avail. BADA type	4.1	3.6

For comparability, both freighters are loaded with 70.000 kg payload and 70.000 kg fuel.

From differences in airplane characteristics (compare Table 1) follows a completely different behavior of both aircrafts. With COALA, these differences can be shown and an optimum trajectory with respect to either minimum fuelburn, minimum time of flight or minimum emissions can be estimated. Thereby, the cruising altitude p_{cruise} and the proportional speed adjustment α act as variable and aerodynamical flight envelopes (i.e. boundaries of c_A , MMO , service ceiling, MTO and MCL) are always respected. Figure 1 shows the profile of both aircrafts for trajectories with minimum time (solid) and minimum fuel (dashed).

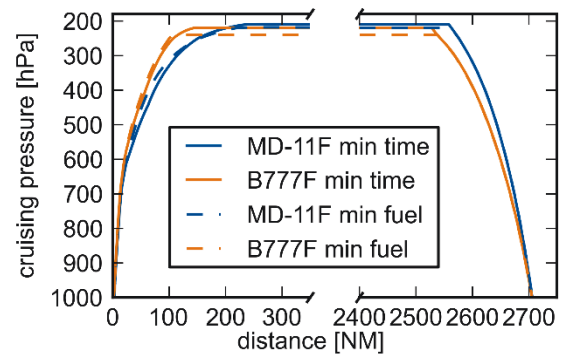


Figure 1: Pressure altitude of the optimized trajectories of both aircrafts. The MD-11F flies with a shallow climb profile and reaches higher cruising altitudes.

3.1. Aircraft specific differences

Although the B777F has more power than the MD-11F (approx. 180 kN, Table 1, Figure 3), the aircraft has difficulties to reach high cruising altitudes of $p_{cruise} = 210$ hPa and higher during the relatively short route (approx. 5000 km, 2700 NM). This phenomenon can be explained by a higher operating empty weight (approx. 30 t, Table 1).

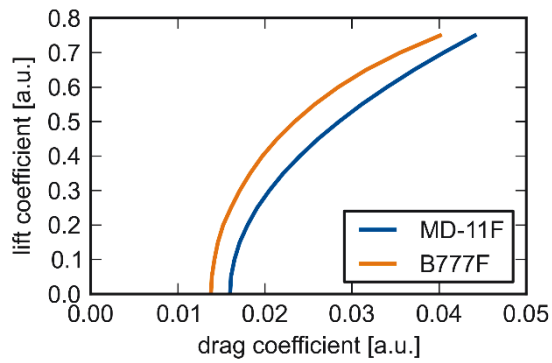


Figure 2: Polar plot of both aircrafts, modeled with BADA 3.6 [8] (MD-11F) and BADA 4.1 [7] (B777F) at Mach=0.7. Higher drag forces are acting on the MD-11F.

However, the simulated cruising altitudes seem realistic, considering the take-off weight of $TOW_{B777F} = 285150$ kg. The B777F climb angle is steeper (compare Figure 1), because of a lower drag polar (Figure 2) and more available thrust (Figure 3), compared to the MD-11F. The B777F descent angle is shallower (Figure 1), due to the lower drag polar.

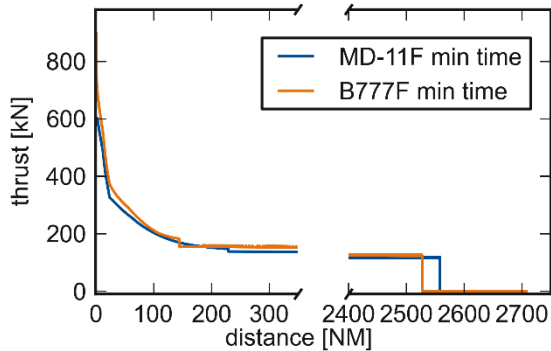


Figure 3: Thrust during optimized trajectories with respect to minimum time of flight of the MD-11F (blue) and the B777F (orange). The B777F offers more thrust.

The higher *OEW* and the lower drag polar cause lower target values of v_{TAS} (compare Figure 4), combined with a steeper climb angle, for the B777F, because an increased gain in altitude (i.e. a larger angle of attack) is possible and causes less drag forces than for the MD-11F. Therewith, the target function of maximum climb rate w reaches higher values of w at the expense of v_{TAS} . For both aircrafts, the target value of v_{TAS} is bordered due to $MMO = 0.87$. Due to the higher *OEW* of the B777F, this speed restriction is more common at MD-11F, than B777F, especially during cruise.

All these differences have to be considered carefully and critically, because two different BADA models with different functional relationships are used. For example, in BADA 4.1, the drag polar and the fuel flow depending on altitude are functions of Mach number. Furthermore, in case of BADA 3.6 [8], maximum cruise thrust is $MCRZ = 0.95 \cdot MCL$, in BADA 4.1 [7], $MCRZ$ is equal to MCL .

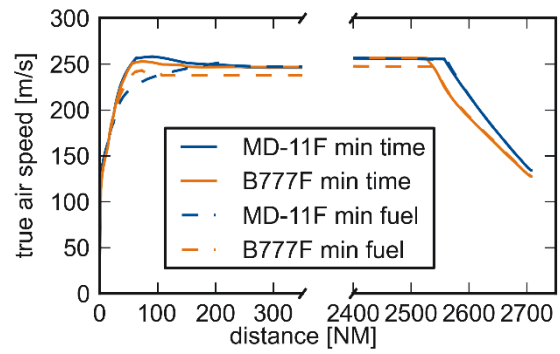


Figure 4: True air speed of the optimized trajectories of both aircrafts. Due to the lower *OEW*, the MD-11F (orange) is faster, especially during climb and descent.

3.2. Trajectory optimization

For trajectory optimization, the cruising altitude p_{cruise} and the speed correction factor α act as free variable. Both variables mainly influence the trajectory (compare Figure 5 to Figure 8). The cruising altitude p_{cruise} was varied 260 – 180 hPa and determines the ambient air density, which influences F_A , F_W , MCL and $MCRZ$. In general, air density decreases with altitude, causing a decrease in all mentioned parameters. Under real weather conditions, altitude dependent wind manipulates the ground speed and therewith the time of flight. These effects are poorly predictable without knowing the change in wind direction and wind speed with altitude. With the variable α (varied 0.9 – 1.12), the true air speed and the climb gradient are manipulated. A target speed v_{TAS} larger than the speed for maximum specific range causes a shallower climb gradient, because more energy is converted into kinetic energy. Hence, time of flight is reduced and fuelburn is increased. An increased v_{TAS} in the target function by the speed correction factor α does not lead to higher cruising altitudes for the B777F, although the aircraft has already burned more fuel by reaching the top of climb. Table 2 shows the results of the trajectory optimization. As expected, minimum time of flight is reached with $\alpha > 1$, at relatively high cruising altitudes, where F_W is reduced. In general, fuelburn and v_{TAS} are less for the B777F resulting in a long time of flight. Pressure altitude and v_{TAS} for these optimized trajectories can be taken from Figure 1 and Figure 4.

Table 2: Optimized variables cruising pressure altitude p_{cruise} and speed correction factor α with corresponding results of time of flight and fuelburn for different objectives of optimization.

Objective	Parameter	MD-11F	B777F
Min. time	p_{cruise}	210 hPa	220 hPa
	α	1.12	1.10
	Time of flight	19461 s	19667 s
Min. fuelburn	p_{cruise}	220 hPa	240 hPa
	α	0.94	1.01
	Time of flight	19537 s	20403 s
	Fuelburn	44816 kg	41151 kg

The effects of different cruising pressure altitudes and speed correction factors are detectable in Figure 5 to Figure 6. Here, fuelburn is calculated for different cruising pressure altitudes and speed correction factors. A large influence of the speed correction factor is simulated for the B777F, partly because the target value of v_{TAS} is often restricted for the MD-11F, to not exceed the maximum Mach number. Furthermore, the optimized variables for trajectories with minimum fuelburn and minimum time can be estimated with the help of Figure 5 to Figure 8.

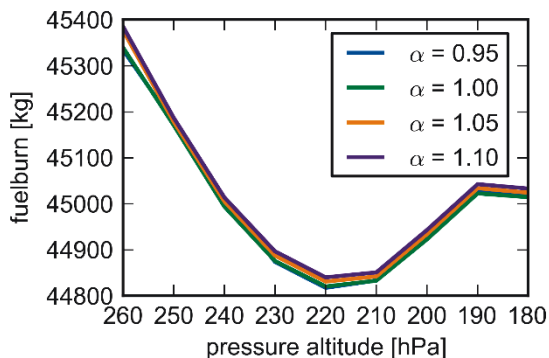


Figure 5: Small influence of speed correction factor α on fuelburn for different cruising pressure altitudes for the MD-11F aircraft. Minimum fuelburn is reached at $p_{cruise} = 220$ hPa and $\alpha = 0.94$.

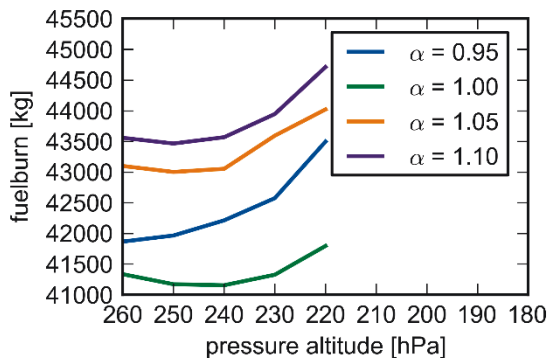


Figure 6: Strong influence of speed correction factor α on fuelburn for different cruising pressure altitudes for the B777F aircraft. Minimum fuelburn is simulated at $p_{cruise} = 240$ hPa and $\alpha = 1.01$.

Figure 7 and Figure 8 show the influence of speed correction factor and cruising pressure altitude on time of flight. For the MD-11F aircraft the influence of the speed correction factor α is limited by maximum Mach number (differences of 9 min in Figure 7 at $p_{cruise} = 260$ hPa), although the model allows a greater range of variation in α . For the B777F, the impact of α on time of flight is significant (differences of 30 min are reached in Figure 8), compared to the impact of cruising pressure altitude.

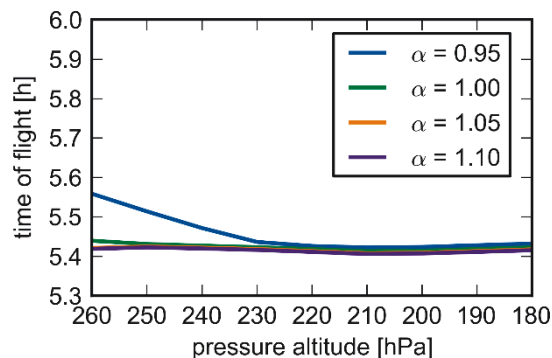


Figure 7: Decreasing impact of speed correction factor α on time of flight with increasing cruising pressure altitude and weak influence of cruising pressure altitude for the MD-11F aircraft due to bordered true air speed above maximum Mach number. Minimum time of flight is reached at $p_{cruise} = 210$ hPa and $\alpha = 1.12$.

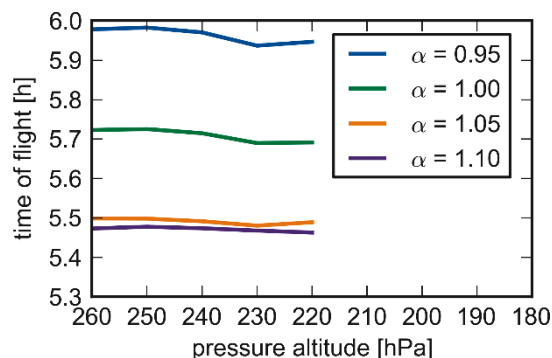


Figure 8: Strong impact of speed correction factor on time of flight and weak influence of cruising pressure altitude on time of flight for the B777F aircraft. Minimum time of flight is reached at $p_{cruise} = 220$ hPa and $\alpha = 1.1$.

Considering the B777 F, it is particularly noticeable, that even for a fuel minimum trajectory the target function for the true air speed should be larger than for the maximum specific range v_{TAS,R_spec} (i.e. $\alpha = 1.01$), although, theoretically, with v_{TAS,R_spec} a maximum gain in kinetic energy per mass of burned fuel is reached.

4. CONCLUSION AND OUTLOOK

The aircraft performance model COALA can calculate and optimize 4D trajectories. The dynamic equation is solved analytically. Therewith, COALA is based solely on physical functions, except for the drag polar, which is approximated by using BADA data. That's why, COALA contains the "limited accuracy" in its name. COALA can model trajectories for several aircraft types, aircraft specific behavior can be modeled in detail. For trajectory optimization, the cruising altitude and the speed correction factor had been identified as effective variables. The developed target function for v_{TAS} (e.g. for a maximum climb rate w or a maximum specific range R_{spec}) can not be generalized for all aircraft types, especially not under real weather conditions. Individual aircraft specific target

functions mainly depend on the drag polar, maximum Mach number and operating empty weight.

In this paper, the results of the included emission model and the possibilities of multicriterial trajectory optimization have not been shown, because the priority was given to the characteristics of COALA and its ability to simulate aircraft specific differences in the flight performance and trajectory optimization. COALA has already been used for multicriterial trajectory optimization in cooperation with TOMATO [1] [5]. Therefore, the performance indicators have been transformed into costs. However, these cost functions would have exceeded the scope of this paper.

COALA uses target functions for the trajectory design and calculates the 4D trajectory for fixed time steps $dt = 1$ s. For the definition of the Shared Business Trajectory (SBT) and the Reference Business trajectory (RBT) due to communication with the air traffic stakeholders the optimized 4D trajectory may have to be converted into way points. However, targeted functions will always be closer to the optimum, especially under consideration of external influences. Without waypoints, the trajectory will not be predictable and difficult to control by Air Traffic Control (ATC). The flight performance model COALA will give all stakeholders the possibility to calculate the desired 4D trajectory and to investigate it with respect to conflicts with other stakeholders. For the RBT, ATC has to release the target function, not the waypoints.

Although free routes require a specified airspace and ATC support tools, some enhanced en-route airspace structures are already addressed in the "Deployment Baseline" along the "SESAR Path to the Target Operational Concept". Here, multiple route options, modular temporary airspace structures, reserved areas and the first steps towards a flexible sectorisation management are focussed [3]. Hence, the need of free routes has been recognized and measures for the implementation had been developed.

A validation of COALA is planned with FODA data from MD-11F and B777F given by Lufthansa Cargo AG. Thereby, the given waypoint based real trajectory has to be transformed into a target function for the aspired v_{TAS} . This process is not possible without errors. Further difficulties are expected due to missing weather data.

5. ACKNOWLEDGMENTS

This work is part of the research project MEFUL, financed by the Federal Ministry for Economic Affairs and Energy (BMWi).

6. REFERENCES

- [1] J. Rosenow, M. Lindner und H. Fricke, „Assessment of air traffic networks considering multi-criteria targets in network and trajectory optimization,“ in *Deutsche Gesellschaft für Luft- und Raumfahrt (DGLR)*, Rostock, 2015.
- [2] SES Single European Sky, „Verordnung (eg) Nr. 549/2004 des europäischen Parlaments und des Rates vom 10. März 2004 zur Festlegung des Rahmens für die Schaffung eines einheitlichen europäischen Luftraums,“ *Rahmenverordnung*, 2004.
- [3] SESAR, „European ATM Masterplan,“ Eurocontrol/SESAR, 2012.
- [4] A. Abeloos, M. von Paassem und M. Mulder, „An Abstraction Hierarchy and Functional Model of Airspace for Airborne Trajectory Planning Support,“ in *Conference on human decision making and manual control*, Linköping University, June 2003.
- [5] J. Rosenow, S. Förster, M. Lindner und H. Fricke, „Multi-objective trajectory optimization,“ *International Transportation (68)*, 2016.
- [6] Lufthansa Systems, „<https://www.lhsystems.com/solutions-services/operations-solutions/lidoflight>“.
- [7] EUROCONTROL, (*BADA*) *Base of Aircraft Data; 4, User Manual Family*, 2012.
- [8] EUROCONTROL, „User manual for the base of aircraft data (BADA) Revision 3.6,“ *EEC Note No. 10/04*, 2004.
- [9] M. Kaiser, Optimierung von Trajektorien strahlgetriebener Verkehrsflugzeuge bei konkurrierenden SESAR Zielfunktionen mittels Entwicklung eines hochpräzisen Flugleistungsmodells, Dresden: Dissertation, Technische Universität Dresden, 2015.
- [10] M. Kaiser, M. Schultz und H. Fricke, „Automated 4D Descent Path Optimization using the Enhanced Trajectory Prediction Model (ETPM),“ in *International Conference on Research in Airport Transportation (ICRAT)*, Berkeley, 2012.
- [11] M. Kaiser, J. Rosenow, M. Schultz und H. Fricke, „Tradeoff between optimum altitude and contrail layer to ensure maximum ecological en-route performance using the Enhanced Trajectory Prediction Model (ETPM),“ London, 2012.
- [12] J. Rosenow, M. Kaiser und H. Fricke, „Modeling Contrail life cycles based on highly precise flight profile data of modern aircraft,“ in *International Conference on Research in Airport Transportation (ICRAT)*, Berkeley, 2012.
- [13] M. Kaiser, M. Schultz und H. Fricke, „Enhanced Jet Performance Model for High Precision 4D Flight Path Prediction,“ Barcelona, 2011.
- [14] M. Schultz, H. Fricke, M. Kaiser, T. Kunze, J. L. Leonés, M. Wimmer und P. Kappertz, „Universal Trajectory Synchronization for Highly Predictable Arrivals Enabled by Full Automation,“ Toulouse, 2011.
- [15] M. Soler, B. Zou und M. Hansen, „Flight trajectory design in the presence of contrails: Application of a multiphase mixed-integer optimal control approach,“ *Transportation Research Part C*, 2014.
- [16] B. Sridhar, H. Ng und N. Chen, „Aircraft trajectory Optimization and Contrails Avoidance in the Presence of Winds,“ *Journal of Guidance, Control, and Dynamics*, 2011.
- [17] R. S. F. Patrón, R. M. Botez und D. Labour, „Flight Trajectory Optimization through Genetic Algorithms Coupling Vertical and Lateral Profiles,“ in *ASME 2014 International Mechanical Engineering*

- Congress & Exposition*, Montreal, 2014.
- [18] A. Murieta Mendoza und R. Mihaela Botez , „Vertical Navigation Trajectory Optimization Algorithm For A Commercial Aircraft,“ in *American Institute of Aeronautics and Astronautics*, 2014.
- [19] U. Ringerz, „Aircraft Trajectory Optimization as a Wireless Internet Application,“ *Journal of Aerospace Computing, Information, and Communication*, 2004.
- [20] R. Howe-Veenstra, „Commercial Aircraft Trajectory Optimization and Efficiency of Air Traffic Control Procedures,“ *Master thesis, University of Minnesota* , 2004.
- [21] C. Hargraves und S. Paris, „Direct Trajectory Optimization Using Nonlinear Programming and Collocation,“ *Journal of Guidance Control and Dynamics*, 1987.
- [22] M. Bittner und B. Fleischmann, „Optimization of ATM Scenarios Considering Overall and Single Costs,“ in *6th International Conference on Research in Air Transportation*, 2014.
- [23] C. Göttlicher, M. Gnoth, M. Bittner und F. Holzapfel, „Aircraft Parameter Estimation Using Optimal Control Methods,“ in *AIAA Atmospheric Flight Mechanics Conference*, 2016.
- [24] V. Grewe, C. Frömming, S. Matthes, S. Brinkop, M. Ponater, S. Dietmüller, P. Jöckel, H. Garny, E. Tsati, K. Dahlmann, O. A. Søvde, J. Fuglestedt, T. K. Berntsen, K. P. Shine, E. A. Irvine, T. Champougny und P. Hullah, „Aircraft routing with minimal climate impact: the REACT4C climate cost function modelling approach (V1.0),“ *Geosci. Model Dev.*, 7, p. 175–201, 2014.
- [25] J. A. Lovegreen und J. R. Hansman, „Estimation of potential aircraft fuel burn reduction in cruise via speed and altitude optimization strategies,“ MIT International Center for Air Transportation (ICAT) , Cambridge, 2011.
- [26] A. Skowron, D.S. Lee und R. R. De León, „Variation of radiative forcings and global warming potentials from regional NOx emissions,“ *Atmospheric Environment* 104, pp. 69-78, 2015.
- [27] O. A. Søvde, S. Matthes, A. Skowron und D. Iachetti, „Aircraft emission mitigation by changing route altitude: A multimodel,“ *Atmospheric Environment* 95, pp. 468-479, 2014.
- [28] J. Scheiderer, *Angewandte Flugleistung*, Springer-Verlag Berlin Heidelberg, 2008.
- [29] National Weather Service, „<http://nomads.ncep.noaa.gov/>,“ 20.02.2016.
- [30] D. Lee, G. Pitari, V. Grewe, K. Gierens, J.E. Penner, A. Petzold und M.J. Prather, „Transport impacts on atmosphere and climate: Aviation,“ *Atmospheric Environment*, p. 4678–4734, 2010.
- [31] A. Kugele, F. Jelinek und R. Gaffal, „Aircraft Particulate Matter Emission Estimation through all Phases of Flight,“ EUROCONTROL Experimental Centre, 2005.
- [32] M. Schaefer, „Methodologies for Aviation Emission Calculation- A comparison of alternative approaches towards 4D global investigations,“ Diploma Thesis , Berlin University of Technology, 2006.
- [33] ICAO, „ICAO Engine Exhaust Emissions Databank Doc 9646- AN/943,“ version 02/2016.
- [34] S. Clark und R. Dogde, *A Handbook for the rolling resistance of pneumatic tires*, Industrial development division, Institute of Science and Technology, The university on Michigan, 1979.
- [35] International Civil Aviation Organization (ICAO), „Continuous Climb Operations (CCO) Manual,“ *Doc 9993 AN/495*, 2013.
- [36] J. Anderson, *Introduction to flight*, New York: McGraw Hill Companies, 2012.
- [37] International Civil Aviation Organization (ICAO), „Continuous Descent Operations (CDO) Manual,“ *Doc 9931 AN/476*, 2010.